Effect of zeolite catalyst on the pyrolysis kinetics of multi-layered plastic food packaging

Kremer, Irma; Tomić, Tihomir; Katančić, Zvonimir; Hrnjak-Murgić, Zlata; Erceg, Matko; Vecchio Ciprioti, Stefano; Schneider, Daniel Rolph

symmetry

MDPI

Article

Effect of Zeolite Catalyst on the Pyrolysis Kinetics of Multi-Layered Plastic Food Packaging

Irma Kremer [1,*], Tihomir Tomić [1], Zvonimir Katančić [2], Zlata Hrnjak-Murgić [2], Matko Erceg [3], Stefano Vecchio Ciprioti [4,*] and Daniel Rolph Schneider [1]

1 Faculty of Mechanical Engineering and Naval Architecture, University of Zagreb, Ivana Lučića 5, 10 002 Zagreb, Croatia; tihomir.tomic@fsb.hr (T.T.); daniel.schneider@fsb.hr (D.R.S.)
2 Faculty of Chemical Engineering and Technology, University of Zagreb, Marulićev trg 19, 10 000 Zagreb, Croatia; katancic@fkit.hr (Z.K.); zhrnjak@fkit.hr (Z.H.-M.)
3 Faculty of Chemistry and Technology, University of Split, Ruđera Boškovića 35, 21 000 Split, Croatia; merceg@ktf-split.hr
4 Department of Basic and Applied Engineering, Sapienza University of Rome, Via del Castro Laurenziano 7, I-00161 Rome, Italy
* Correspondence: irma.kremer@fsb.hr (I.K.); stefano.vecchio@uniroma1.it (S.V.C.)

Abstract: Pyrolysis is gaining more significance as a technology used to produce alternative fuels and chemicals. This study dealt with the catalytic pyrolysis of a realistic waste mixture of multi-layered plastic food packaging. The thermal behavior, kinetic parameters, and kinetic model of multi-layered plastic food packaging pyrolysis were determined to show its potential for process scale-up. In particular, we aimed to evaluate the effect of a ZSM-5 zeolite catalyst, modified with iron(III) oxide. The pyrolysis process on this decagonal structure was investigated using thermogravimetric analysis under nitrogen flow at four heating rates ranging between 40 and 600 °C. The kinetic study was conducted using the model-free isoconversional Friedman method as well as advanced statistical analysis to determine the reaction mechanism of the process. The thermal decomposition occurred in the range of 350–510 °C, with a mass loss greater than 90%. The kinetic study revealed a complex pyrolysis process, which consisted of three decomposition stages, diffusion, and Avrami-Erofeev reaction types. The activation energy values determined by the Friedman method rose with the degree of conversion, from 127 kJ mol^{-1} at 0.01 to 219 kJ mol^{-1} at 0.95. The doping of the catalyst lowered the activation energy of the reaction by 44% and 8% in the first and second stages, respectively, and increased the acidity of the zeolites, thus enhancing the reactivity on the surface of the catalysts. Lower activation energy meant less energy was required to heat the pyrolysis reactor since the onset temperature of sample decomposition was reduced.

Keywords: zeolite catalyst; pyrolysis; multi-layered plastics; food packaging; thermogravimetric analysis; kinetic study

Citation: Kremer, I.; Tomić, T.; Katančić, Z.; Hrnjak-Murgić, Z.; Erceg, M.; Vecchio Ciprioti, S.; Schneider, D.R. Effect of Zeolite Catalyst on the Pyrolysis Kinetics of Multi-Layered Plastic Food Packaging. *Symmetry* **2022**, *14*, 1362. https://doi.org/10.3390/sym14071362

Academic Editors: Bozhidar Stefanov, İlknur Bayrak Pehlivan and Silvia Todorova

Received: 8 June 2022
Accepted: 28 June 2022
Published: 1 July 2022

1. Introduction

Multi-layered plastic food packaging (MPFP) consists of polymers that are combined to provide optimum packaging quality. The use of MPFP is expanding, and this growth is expected to continue [1]. Today, 40% of the 55 Mt of plastics produced in Europe are used for packaging [2]. MPFP accounts for up to 17% of total plastic packaging film manufacturing [3]. MPFP is characterized by functional, protective, and decorative characteristics that are the outcome of combining layers of thermoplastics. MPFP is largely used in the food market to preserve the quality of products while ensuring minimal food waste, which accounts for around 30% of the overall production of food [4]. The total thickness of MPFP varies from 30 µm to 1 mm and is determined by the number of layers, which can range from 3 to 20 [5]. In addition, the layers may include adhesives, metals, or printing ink, which are frequently much thinner than the primary layers and are not

always employed [6]. Therefore, they are not discussed in this study. The purposes of layers are different. A certain layer can serve as a gas barrier, water barrier, structural support, resistance to abrasion, or a sealable or printable material [7].

Using diverse materials with different functions reduces the average thickness of packaging [8]. Consequently, unnecessary material consumption and associated costs are avoided [9]. Nonetheless, the diverse composition of MPFP makes mechanical recycling difficult [10].

Currently, recycling MPFP is difficult due to the inability of contemporary technology to identify and separate its component layers, while waste treatment facilities to classify, segregate, and recycle MPFP have not yet been established [11,12]. Therefore, it is typically separated as heterogeneous waste plastic and frequently incinerated for energy in EU states [11]. In financially disadvantaged areas, heterogeneous waste is disposed of predominantly in landfills [13]. The EU favors energy recovery by incineration over landfilling [14]. However, compared to disposal in landfills, incineration might be worse for socioeconomic sustainability [15]. The most current, thorough review research on the recycling of MPFP stated that its future depends on the advancement of waste treatment technologies, particularly in nations with high incomes. First, the sorting process must be improved to ensure the highest quality of the recovered product. The study identified thermochemical recycling (feedstock) as the most recommended alternative approach [16], which comprises pyrolysis, gasification, fluid-catalyzed cracking, and hydrocracking [17]. There is the possibility for pyrolysis becoming an effective solution for depolymerizing difficult-to-depolymerize plastic waste, such as MPFP [18]. The outputs of pyrolysis are valuable substances that can be further processed, such as oil, gas, and char [19]. This study concentrates on pyrolysis as MPFP recycling technology. The products of pyrolysis can be selectively generated using catalysts [20]. One of the most used catalysts in plastic pyrolysis are zeolites. One study examined the optimal ratio of ZSM-5 zeolite to MCM-41 catalyst to ensure the best conversion rate of the waste plastic to gasoline-range hydrocarbons [21]. Another one studied the influence of zeolite catalysts (y-zeolite, β-zeolite, and ZSM-5) on the composition of pyrolysis oil obtained from End of Life Vehicles' plastic waste [22]. USY zeolite was used to obtain diesel- and gasoline-like fuels from polyolefins pyrolysis [23].

The research on catalytic pyrolysis of MPFP is relatively new. In all currently available studies on this topic, zeolites were used as the catalyst. In the majority of the studies, the products of catalytic pyrolysis were analyzed, while the pyrolysis kinetics was not taken into account [24–26]. One of the studies that focused on the pyrolysis of waste coffee packaging of known materials used a combination of thermogravimetry (TG) and gas chromatography-mass spectrometry (GC-MS) [24]. Another one examined the catalytic pyrolysis of different MPFP samples with specified composition using iron-doped zeolite that resulted in pyrolytic oil and carbon nanotubes [25]. In another one, a pilot-scale batch reactor was employed to test the catalytic pyrolysis of various types of polyolefins and MPFP waste, as well as their mixtures. Regarding the ratio of polymer and material of MPFP to polyolefin mixtures, no particular information was provided [26]. A series of studies was done on the pyrolysis and catalytic pyrolysis of MPFP waste that contained aluminum, in addition to an examination of the kinetics of the process [27–29]. The amount of aluminum foil was established, although the content of polymers in these mixtures remains uncertain. The pyrolysis yielded oil, gas, and regenerated aluminum.

The thermal characterization of mixed plastics from packaging and electric equipment residues showed the advantages of applying pyrolysis feedstock recycling from an energetic point of view [30]. All the heat change contributions due to physical and/or chemical processes detected through thermal analysis experiments, defined as the degradation heat and determined for both single component and their mixtures, were found to be about 4–5% of the exploitable energy of the input material. Thermal analysis was also used for the identification and characterization of some thermoplastic components of WEEE when they were subjected to a pyrolysis process [31].

Benedetti et al. [32] found a noticeable improvement in the production of light oil to the detriment of tar by carrying out catalytic pyrolysis of thermoplastics extracted from waste electrical and electronic equipment (WEEE) using various catalysts prepared from fly ash with a simple method that basically included a mechanical treatment followed by an acid or a basic activation. It is notable that the pore dimensions played a fundamental role in the catalytic effect of pyrolysis of WEEE using HUSY and HZSM5 catalysts, which were 5.8, 7.3, and 8 Å for ZSM5, X, and USY zeolites, respectively [33].

On the other hand, a significant yield of the gaseous fraction produced by the thermal pyrolysis was due to the breaking of aliphatic chains in small fragments [34]. Faujasite zeolites typically induced the formation of char due to their large cavity volume where secondary reactions can take place [35].

Previous studies on MPFP pyrolysis generated valuable products [24–29]. However, the focus of these studies was on particular types of MPFP rather than on the total makeup of the waste stream. In some studies, information regarding specific polymer ratios was lacking. It is essential to know the content of the input material so that the other operating variables (temperature, residence time, and catalyst-to-polymer ratio) in the reactor may be adjusted appropriately to produce a high-quality output [36]. During the manual sorting of mechanically non-recyclable post-consumer waste, a large volume of plastic waste labelled as "other" or category 7 plastics (according to the Resin Identification Code system) was discovered in our earlier research [37]. The FTIR analysis was employed to quickly identify polymers and demonstrated that the "other" plastics comprised a minimum of two layers, as the exterior and interior sides of the package were distinct. It was found that PET and PE were present in the outer and inner layers of almost every sample, respectively, while PP was found rarely in the inner layer. Based on a large number of studied waste samples [37], a realistic blend of MPFP with specified polymer ratios was chosen in the present investigation.

The main aim of this study was to examine the role of doping the selected zeolite catalyst with iron(III) oxide in affecting the thermal decomposition and the reaction mechanism (kinetics) of a realistic waste mixture of MPFP undergoing pyrolysis. This was accomplished by conducting TG and kinetic analyses using model-free isoconversional methods and an advanced statistical approach. The collected results are very beneficial for adjusting the operating conditions of the scaled-up process.

2. Materials and Methods

2.1. Materials

Our previous investigations of real-world MPFP showed that it mainly consisted of polymers PET, PE, and PP, and it was not quantifiable in a safe way. The usual techniques employed in the quantification and identification of MPFP demand the separation of the polymer layers with solvents such as concentrated acids, tetrahydrofuran, dimethyl sulfoxide, toluene, xylene and ethyl acetate. Therefore, in our previous study, we contacted the largest producer of MPFP in Croatia to obtain the most common samples that were found during MPFP waste analysis. Those samples were containers for fresh meat and quick-prep food, various snacks, and frozen food packaging [37]. The representative samples were collected from the company together with the data about the shares of polymers in the products and their typical usage. An equal amount of each sample presented in Table 1 was added to prepare the investigated realistic MPFP waste mixture, which comprised 71.9% PET, 25.1% PE, and 3.0% PP. Each sample was cut into small pieces, with a size of 2–3 mm. The metallization of foils was done using a plasma metallization process, resulting in very fine particles that could not be measured in μm.

A powdered ZSM-5 zeolite catalyst defined by the MFI (Mobil Five) crystal structure (Grace, Worms, Germany) and loaded with iron (III) oxide was used in these experiments. The properties and characterization of the synthesized catalyst were described in a previous study [37]. Some of the main characteristics of the catalyst are a pore diameter ranging

from 2.5 to 5 nm, a surface area of 135 m^2 g^{-1}, an average particle size of 82 μm and a SiO_2/Al_2O_3 ratio of 4.07.

Table 1. Characteristics of the selected samples.

No.	Composition	Thickness/μm	PET/PE/PP/%	Description and Use
1	APET/PE	450/50	90.0/10.0/0	Transparent rigid film used in fresh meat, salami, and quick-prep food packaging
2	PET/boPP metallized	12/20	37.5/0/62.5	Metallized flexible film used in snacks and sweets packaging
3	PET/PE metallized	12/45	21.1/78.9/0	Metallized flexible film used in snacks packaging and frozen food packaging
4	PET/PE laminated	12/75	13.8/86.2/0	Transparent flexible film used in frozen food and sour vegetable packaging
5	Mixture	-	71.9/25.1/3.0	-

2.2. Thermogravimetry

A thermogravimetric analyzer Q500 (TA Instruments, DE, USA) was used to perform the pyrolysis experiments. The measurements were performed in an inert atmosphere (nitrogen) with a flow of 60 cm^3 min^{-1} at multiple heating rates (5, 10, 15, and 20 °C min^{-1}) ranging between 40 and 600 °C. The mixture contained 1.5 mg of each sample, with 6 mg in total per experiment. The catalyst loading was 15%.

2.3. Kinetic Study

The purpose of this study's kinetic investigation was to see how the catalyst affected the thermal degradation of MPFP. Plastics' thermal breakdown is a solid-state process. Equation (1) can be used to express the rate of a single-stage solid-state reaction:

$$d\alpha/dt = \beta\, d\alpha/dT = A \exp(-E/RT)\, f(\alpha), \quad (1)$$

where α is the degree of conversion, t is the time, β the linear heating rate (°C min^{-1}), A is the pre-exponential factor (min^{-1}), E is the activation energy (kJ mol^{-1}), R is the universal gas constant (J mol^{-1} K^{-1}), T is the absolute temperature (K), and $f(\alpha)$ is the kinetic model function. The fundamental kinetic equation that describes the overall process is Equation (1). The kinetic triplet, namely, E, A and $f(\alpha)$, can describe the reaction mechanism and was calculated from experimental data. The percentage of total mass loss in the process is represented by an overall degree of conversion. The total conversion may include more than one reaction or, more accurately, numerous reactions, each with its own conversion degree. As a result, the International Confederation for Thermal Analysis and Calorimetry (ICTAC) [38] advises using kinetic methods that can identify reactions with multiple stages. Equation (2) can be used to calculate the fraction of mass loss (pyrolysis conversion):

$$\alpha\,(T) = (m_0 - m_T)/(m_0 - m_f), \quad (2)$$

where m_0 and m_f are the initial and the final sample masses, while m_T is the sample mass at a temperature T during the occurrence of pyrolysis.

The following steps should be taken to identify the best kinetic model from the experimental results [38,39]:

1. Record the TG measurements performed at different heating rates (at least 4 or 5). The shapes of the TG and DTG (first-order derivative of TG data) curves can indicate the reaction path. When the residual mass varies with the heating rate, it usually indicates branching in the reaction path; otherwise, the reaction path remains unbranched.
2. Process the experimental TG data to calculate the activation energy associated with degradation steps by isoconversional methods. According to ICTAC's guidelines,

a kinetic study should start with the precise determination of one parameter without any assumption of a kinetic model (a mechanism). Model-free isoconversional approaches make this achievable. Isoconversional model-free approaches such as those of Ozawa–Flynn–Wall and Kissinger–Akahira–Sunose (integral methods) [40] and Friedman (differential method) [41] are the most commonly utilized methods for kinetic analysis of solid-waste pyrolysis processes. Model-fitting methods are also often used, with the Coats–Redfern method dominating solid-waste pyrolysis research [42,43]. The differential Friedman method was used in this research. Friedman's differential model-free isoconversional method employs the logarithmic form of the fundamental kinetic equation:

$$\ln[\beta\ (\mathrm{d}\alpha/\mathrm{d}T)] = \ln A + \ln f(\alpha) - E/RT. \quad (3)$$

By plotting the left-hand side of Equation (3) against $1/T$ for each constant α value, the activation energy can be calculated using the slope of straight lines.

3. Plot the obtained activation energy against the degree of conversion. If the highest and lowest calculated values of activation energy values vary by more than 30% from the average value, it is implied that the process is complex and occurs in multiple stages [44]. This demands multivariate non-linear model-fitting regression methods. Otherwise, if it does not vary significantly, the process is simple, and the kinetic model can be determined by using linear model-fitting regression methods to the experimental data.
4. Obtain Friedman plots from the experimental data (Equation (3)). It is very important to compare the slopes of the experimental data and isoconversional lines by the Friedman method at the beginning of the reaction ($0.01 < \alpha < 0.10$) since this will give insight into the most probable process at the initial reaction stage:
    a. The slopes are comparably similar: reaction-order or phase-boundary reaction;
    b. The slope of the experimental data is lower than the slope of the isoconversional lines: diffusion;
    c. The slope of the experimental data is steeper than the slope of the isconversional lines: autocatalytically activated reaction type of Avrami–Erofeev.

To determine the best kinetic model, linear or multivariate non-linear regression is used to fit the reaction models to the experimental TG data, depending on the complexity of the process. Netzsch Thermokinetics 3.0 software (Netzsch Group, Selb, Germany) [45] was used to fit well-known solid-state reaction models [38] to experimental data. According to the statistical approaches of the least-squares method and the *F*-test, the best model is the one that provides the smallest discrepancy between the calculated and measured data. In accordance with the *F*-test, the compatibility of the experimental data to the kinetic model is determined as follows:

$$(S_\mathrm{j})^2 = 1/(n-1)\sum_{\mathrm{i}=1}^{\mathrm{n}}[(\mathrm{d}\alpha/\mathrm{dt})_\mathrm{exp} - (\mathrm{d}\alpha/\mathrm{dt})_\mathrm{model}]^2 \quad (4)$$

where $(S_\mathrm{j})^2$ is the variance, n is the number of collected experimental data, and $(\mathrm{d}\alpha/\mathrm{d}T)_\mathrm{exp}$ and $(\mathrm{d}\alpha/\mathrm{d}T)_\mathrm{model}$ are the experimental data and model calculated data, with the latter referring to a certain kinetic model. When the variance values of a single model $(S_\mathrm{j})^2$ are divided by the minimum variance value $(S_\mathrm{min})^2$ of all observed models, the so-called *F*-test and the F_exp value are calculated:

$$F_\mathrm{exp} = (S_\mathrm{j})^2/(S_\mathrm{min})^2 < F_\mathrm{crit} \quad (5)$$

In accordance with the *F*-test, only those models satisfying Equation (5), i.e., those for which F_exp holds $< F_\mathrm{crit}$, are deemed statistically feasible models for describing the studied process. In this study, the value of F_crit was derived from the number of experimental points and the degree of statistical significance, also known as the statistical probability. If

the statistically best model has the greatest agreement with the activation energy estimated by the isoconversional approach ($E \approx E_{FR}$), it can then be considered as a kinetic model of the investigated process [39].

3. Results and Discussion

3.1. Thermogravimetric Analysis

The thermogravimetric (TG) curves (mass loss) recorded at four different heating rates ranging from 5 to 20 °C min^{-1} and the first-order derivative TG curves (DTG, rate of mass loss against temperature) are shown in Figure 1a,b for the investigated mixture. As shown by Vyazovkin et al. [38], each peak or shoulder represents a minimum of one reaction step.

An examination of the TG curves implies that thermal decomposition took place in at least a two-step process between 350 and 510 °C, with a shift to higher temperatures. The first visible DTG peak temperature (actually a shoulder) was found at 417, 428, 439, and 449 °C, depending on the heating rate, while a second DTG shoulder temperature was observed at 445, 458, 468, and 476 °C (Figure 1b). A TG analysis of pure PET showed how it degraded between 375 and 490 °C [46], while PE degraded between 440 and 510 °C and PP degraded between 415 and 510 °C [47].

Hence, the first peak corresponds to PET, and the second peak corresponds to PE and PP. At 10 °C min^{-1}, the value of maximum degradation temperature for pure PET was found to be 438 °C [46]; for PE, it was found to be 473 °C; and for PP, it was found to be 458 °C [47]. Based on the obtained results of the mixture pyrolysis, possible synergistic effects were observed. During the pyrolysis process, the degradation temperature was reduced by 10 °C for PET and by 15 °C for PE. The degradation temperature of PP remained the same. The thermal degradation of both PET and PE was accelerated during the pyrolysis of the investigated mixture. Over 90% of the mass was lost, indicating that the mixture included a great deal of volatile matter. Typically, highly volatile matter enhances liquid oil production [48].

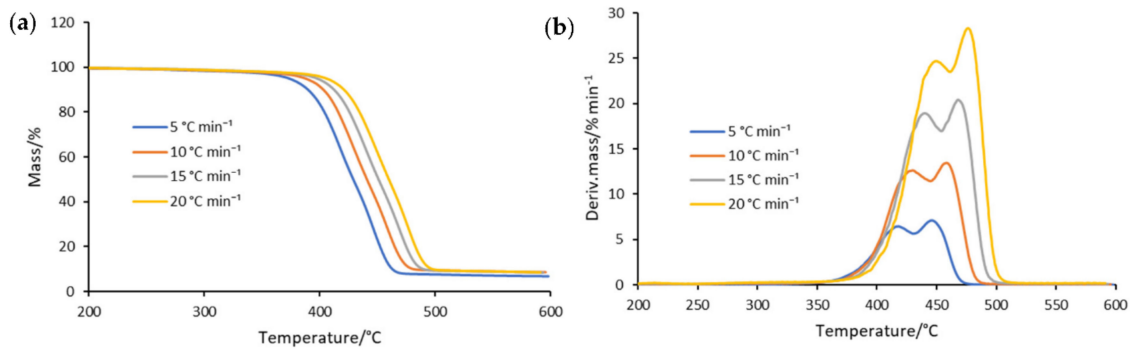

Figure 1. (**a**) TG and (**b**) DTG curves of the plastic mixture recorded under a nitrogen-flowing atmosphere (60 cm^3 min^{-1}) at 5, 10, 15. and 20 °C min^{-1}.

The TG and DTG curves of the individual samples and mixture recorded at 10 °C min^{-1} are compared in Figure 2a,b. The shape of the TG and DTG curves clearly changes depending on the composition of each sample. The change in the residual mass shown in Figure 2a was the most noticeable. A higher content of PET in the sample (Table 1) resulted in higher residual mass after the pyrolysis process. According to the proximate analysis of pure PET, a possible reason for the higher residual mass was the higher ash and fixed carbon content [47]. Figure 2b shows that the sample APET/PE with the highest content of PET degraded in a similar range as pure polymer [46]. Likewise, laminated sample PET/PE, consisting mostly of PE, degraded in a similar range as pure PE, although a small shoulder was still visible at lower temperatures corresponding to the content of PET. Two shoulders were clearly visible in the metallized samples PET/boPP and PET/PE. The first one can be annotated to PET, and the second one to PP and PE [46,47].

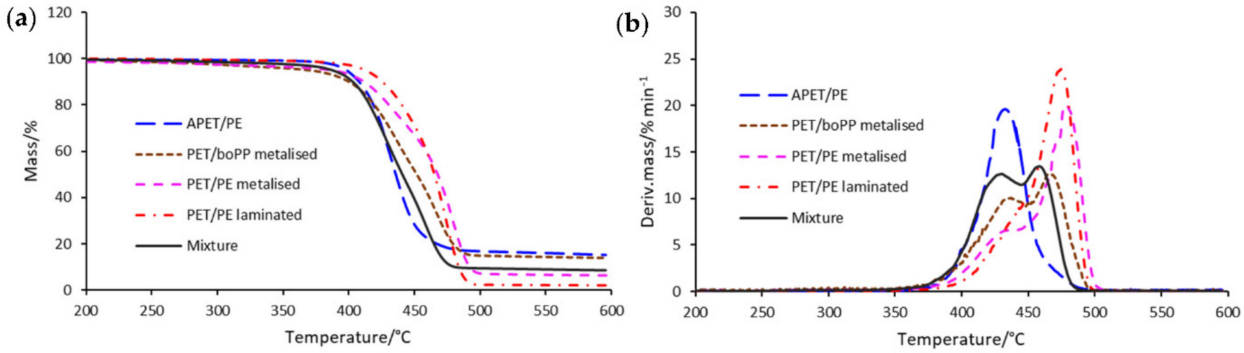

Figure 2. (**a**) Thermogravimetric and (**b**) derivative thermogravimetric curves for the individual samples and mixture at 10 °C min^{-1}.

The effect of the iron-doped ZSM-5 catalyst on the thermal decomposition of each individual sample and mixture was investigated by comparing the corresponding TG and DTG curves performed at 10 °C min^{-1} (Figures 3 and 4).

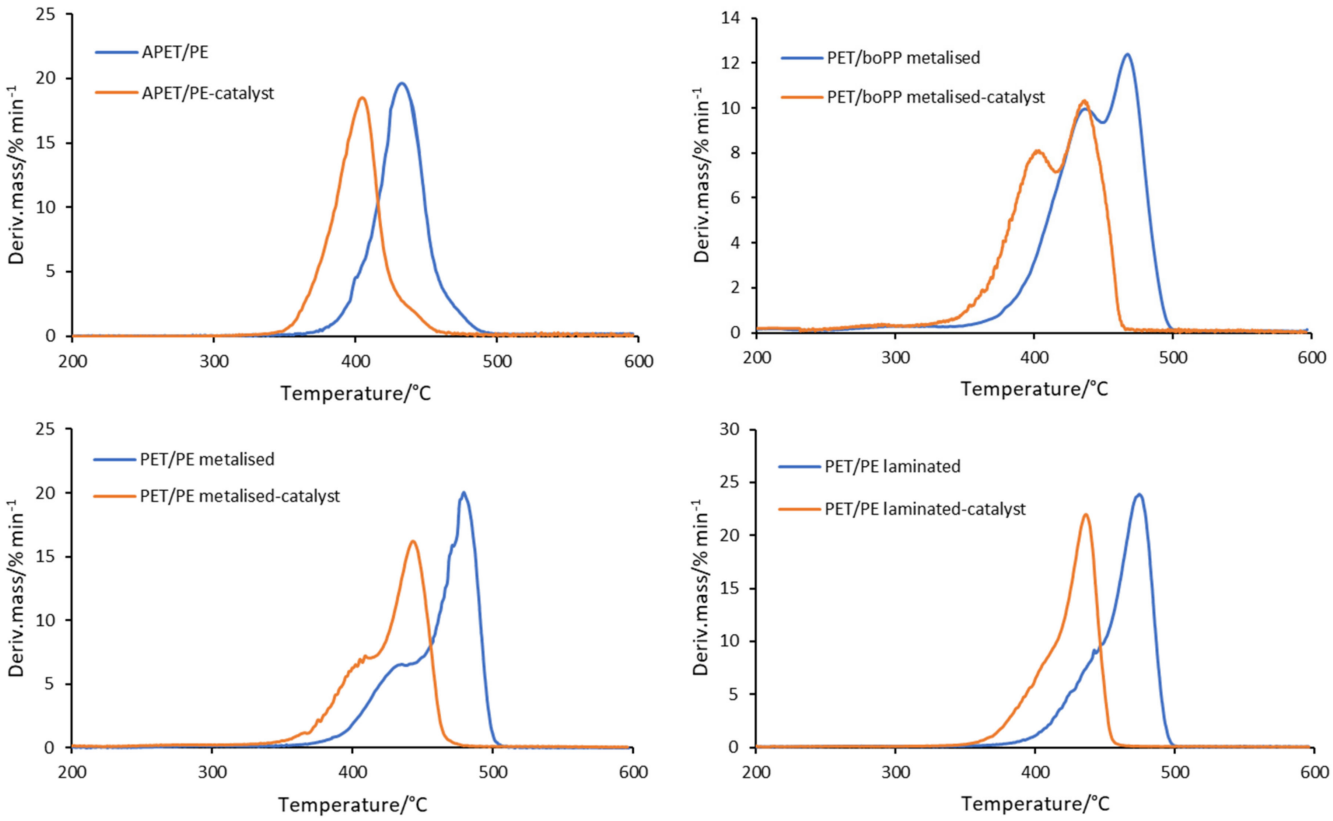

Figure 3. Derivative thermogravimetric curves for the individual samples with the catalyst at 10 °C min^{-1}.

Table 2 displays the onset decomposition temperatures as well the DTG peak temperatures. It is quite evident that these temperatures decreased with the addition of the catalyst. In particular, the temperature shifts ranged from 22 °C to 38 °C (Table 2). Another TG study on MPFP that contained PET, PE, and aluminum also resulted in a shift of decomposition temperature, from 472 °C to 429 °C, with the addition of HZSM-5 zeolite catalyst [24]. A study on TG decomposition of HDPE revealed how a ZSM-5 catalyst lowered the onset decomposition temperature by 120 °C [49].

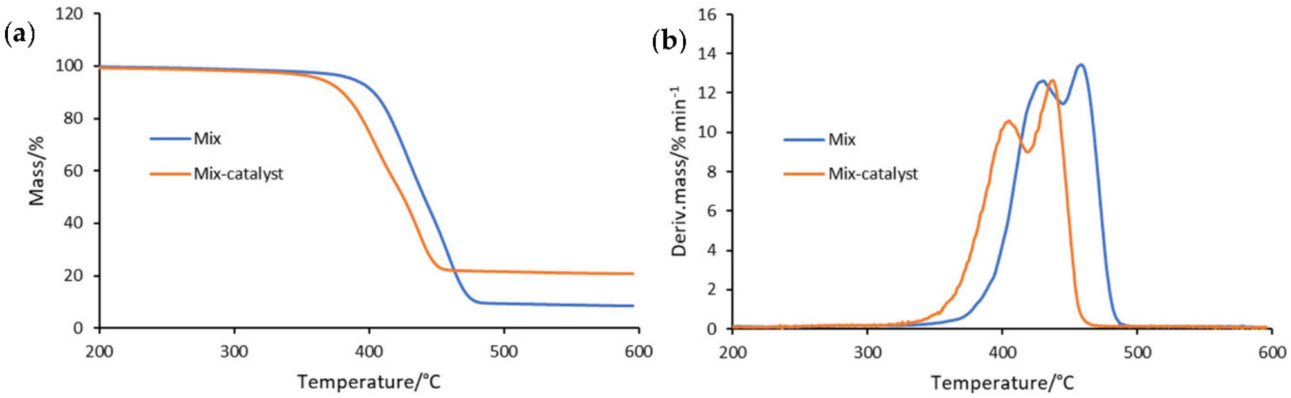

Figure 4. (**a**) Thermogravimetric and (**b**) derivative thermogravimetric curves for the mixture with the catalyst at 10 °C min^{-1}.

Table 2. Thermogravimetric parameters for investigated samples at 10 °C min^{-1}.

No.	Sample	T_{on}/°C	T_1/°C	R_1/% min^{-1}	T_2/°C	R_2/% min^{-1}
1	APET/PE	398	433	19.60	–	–
	APET/PE-catalyst	369	405	18.49	–	–
2	PET/boPP	369	436	10.02	467	12.52
	PET/boPPmet-catalyst	346	406	8.00	438	10.17
3	PET/PEmet	386	433	6.78	478	19.9
	PET/PEmet-catalyst	361	404	6.46	442	16.22
4	PET/PElam	413	–	–	474	23.83
	PET/PElam-catalyst	381	–	–	436	21.96
5	Mix	387	428	12.88	458	13.71
	Mix-catalyst	363	404	10.58	436	12.65

T_{on} = onset temperature at which mass loss began; T_1 = peak temperature of the first step; R_1 = maximum mass loss rate of the first peak; T_2 = peak temperature of the second step; R_2 = maximum mass loss rate of the second peak.

The shapes of DTG peaks of the samples with catalyst were similar to those of the original samples, indicating that the decomposition was accelerated in the presence of a catalyst, with negligible change in the reaction mechanism. The catalyst used in this study [37] had a low SiO_2/Al_2O_3 ratio, which was correlated with higher acidity and high reactivity on the surface when gas–solid processes took place [49]. As a result of this catalyst property, the activation energy of the pyrolytic process decreases, resulting in the decomposition of the sample at lower temperatures and consequently lowering the energy consumption. However, it was also found that a lower SiO_2/Al_2O_3 ratio was associated with higher gas sorption (retention in pores) [50] and somewhat lower mass loss rates. Hence, a slight difference was found between the mass loss rates of the original samples and those of the samples with catalyst. Figure 4a shows that the residual mass was higher in the presence of a catalyst due to the fact that these were inorganic substances commonly known to be very stable at high temperatures.

3.2. Results of the Kinetic Study

Details regarding the procedure for the kinetics computation to find the appropriate kinetic model for the MPFP mixture pyrolysis reaction are reported in sub Section 2.3. As illustrated in Figure 1a, the residual mass of the mixture did not change with the increase in the heating rate. Similar results were obtained in the TG experiments of the mixture with the catalyst. This implied that the reaction path did not branch.

Figure 5 shows the conversion dependence of the activation energy for the decomposition of the mixture with and without the presence of the catalyst, calculated according to the Friedman method (E_{FR}). The presence of the two peaks in the DTG curves of the mixture and the mixture with catalyst indicated at least two decomposition stages (Figures 1b and 4b). This interpretation was supported by the fact that the discrepancy between the calculated maximum and minimum values exceeded 30% of the mean activation

energy value, suggesting that the process was complex and consisted of several steps. The trend of activation energy for the decomposition of the mixture slightly increased, from 127 to 219 kJ mol^{-1}. In the presence of the iron-doped ZSM-5 catalyst, the E_{FR} values of pyrolysis visibly lowered in the conversion range up to 0.4 (Figure 5 and Table 3). Another study on MPFP that consisted of PET, PE, EVA, and aluminum also showed the decrease in the average activation energy calculated by the isoconversional method after the addition of the ZSM-5 zeolite catalyst. The values decreased from 260 kJ mol^{-1} to 178 kJ mol^{-1} at a catalyst loading of 10% [29].

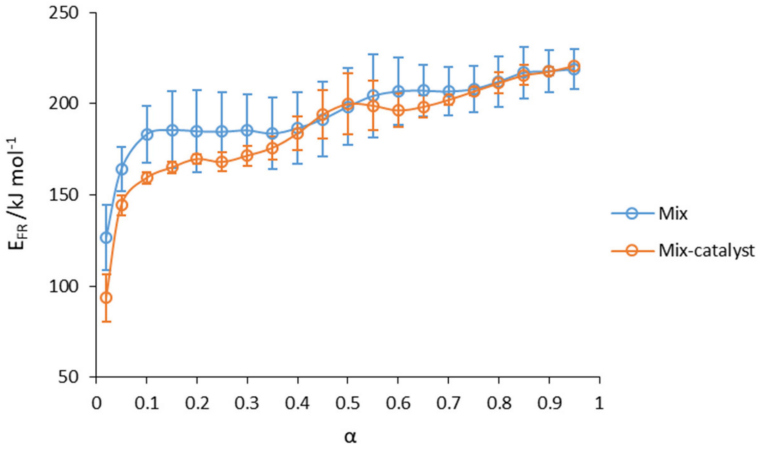

Figure 5. Conversion dependence of E_{FR} on α for the decomposition of the mixture and mixture with the catalyst.

After confirming that pyrolysis is a complex process, the kinetic model at the beginning of the reaction must be estimated (α = 0.01–0.10).

The approach outlined in sub Section 2.3. allowed us to deduce how the initial process corresponded to the diffusion in both cases from the Friedman plots reported in Figure 6a,b. In the ensuing phase of the reaction, two peaks were visible, indicating that two more decomposition processes continued after the occurrence of diffusion. These results suggest that the decomposition took place in three steps, either with or without a catalyst.

After studying Friedman plots and determining that the process involved more than one step, the experimental data were compared with a set of reaction models [38] using a non-linear multivariate model-fitting regression method. The appropriate kinetic model was identified using the *F*-test statistical procedure described in sub Section 2.3. The values of F_{crit} for the process related to the mixture without and with the catalyst were 1.04 and 1.03, respectively. A model that satisfied the criterium $F_{exp} < F_{crit}$ was regarded as the most accurate mechanism (model function) associated with the investigated process. In this instance, the models that met the criterion produced the value F_{exp} = 1.0 for both samples, as shown in Table 3.

Table 3. Kinetic parameters for the mixture and mixture with catalyst: statistical fit and Friedman method values.

Stage of Reaction	Parameter	Mix		Mix-Catalyst	
		Statistical Fit	Friedman	Statistical Fit	Friedman
Stage 1	E1 (kJ mol^{-1})	131.1	143.9	66.4	80.7
	log A1	7.1	8.4	2.2	3.7
	n	–	–	–	–
	Model	D3	–	D3	–
	Conversion range	0.00–0.05		0.00–0.04	

Table 3. *Cont.*

Stage of Reaction	Parameter	Mix		Mix-Catalyst	
		Statistical Fit	Friedman	Statistical Fit	Friedman
Stage 2	E2 (kJ mol^{-1})	200.0	191.9	197.1	177.3
	log A2	12.7	11.8	13.1	11.1
	n	0.69	–	0.82	–
	Model	An	–	An	–
	Conversion range	0.10–0.65		0.05–0.60	
Stage 3	E3 (kJ mol^{-1})	218.6	213.5	213.0	210.5
	log A3	13.1	13.3	13.2	13.6
	n	4.0	–	3.9	–
	Model	An	–	An	–
	Conversion range	0.70–0.95		0.65–0.95	

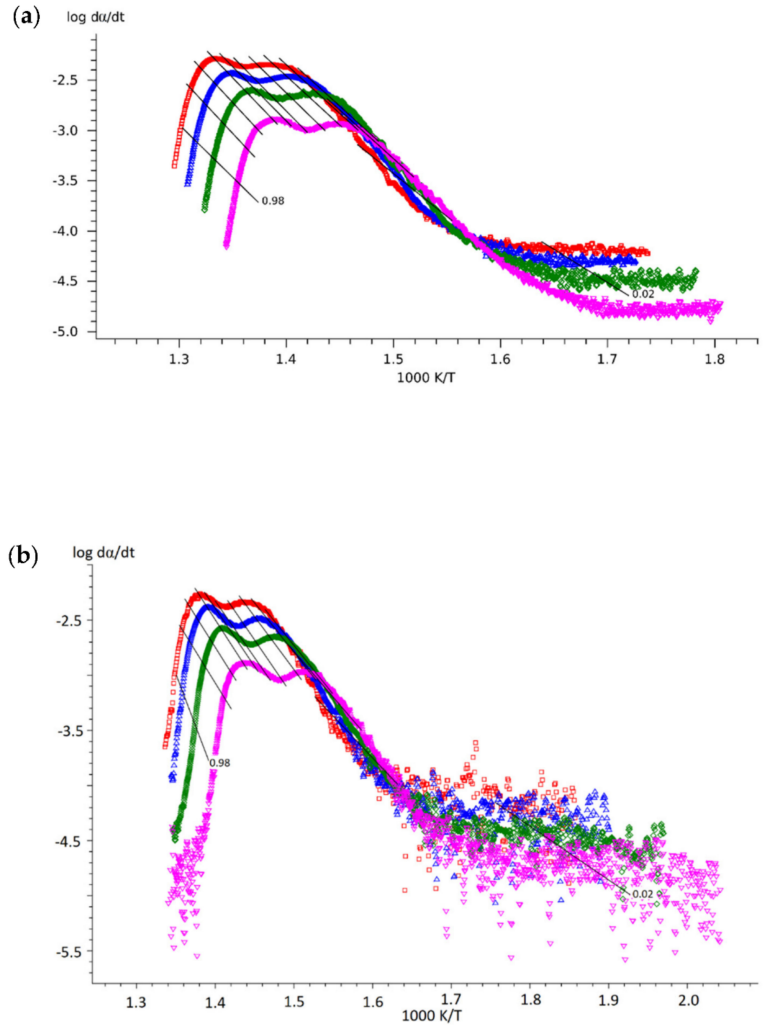

Figure 6. Friedman plots for the non-isothermal decomposition for (**a**) the mixture and (**b**) mixture with the catalyst.

The kinetic parameters determined according to the best statistical fit (E, log A) were compared in Table 3 with those determined by the isoconversional Friedman method (E_{FR}, log A_{FR}). The E values for potential kinetic models correlated to the experimental E_{FR} values, within the experimental error. In accordance with the approach outlined in sub Section 2.3, the derived kinetic models could be applied to identify the researched pyrolysis processes.

The assumptions made based on the form of the TG/DTG curves and Friedman plots of the mixture and mixture with catalyst were supported by the data reported in Table 3. Both samples underwent decomposition in three successive stages. As expected from the Friedman plots of both samples at the start of the reaction, the first one was characterized by diffusion (Jander's type). Furthermore, two additional decomposition steps were annotated in both samples that could be represented by two distinct An models (Avrami–Erofeev reaction type). The catalyst had the greatest effect on the decomposition process of the mixture during the initial stage. ZSM-5 catalysts are typically microporous, and micropores hinder rapid diffusion [20]. However, the iron-doped ZSM-5 catalyst used in this study was mesoporous, thus enhancing the diffusion at the beginning of the process. The doping of the catalysts also increases the acidity of the zeolites [20] and, consequently, the reactivity on the surface of the catalyst [49]. The incorporation of metals in porous structures, i.e., the synthesis of metal–organic frameworks, is known to increase catalytic activity [51]. In the later stages of the process, the iron-doped ZSM-5 catalyst did not significantly induce a decrease in the activation energy for pyrolysis, with the possible reason being the formation of coke within the pores. The use of a macroporous catalyst would reduce the likelihood of coke formation. However, macroporous catalysts are usually weakly acidic and lack contact with polymer active sites [20].

The analyses presented in Figure 7a,b indicate that the experimental and calculated data matched well, where the latter were derived using the kinetic model of the non-isothermal decomposition of the MPFP mixture obtained by the non-linear regression model-fitting method.

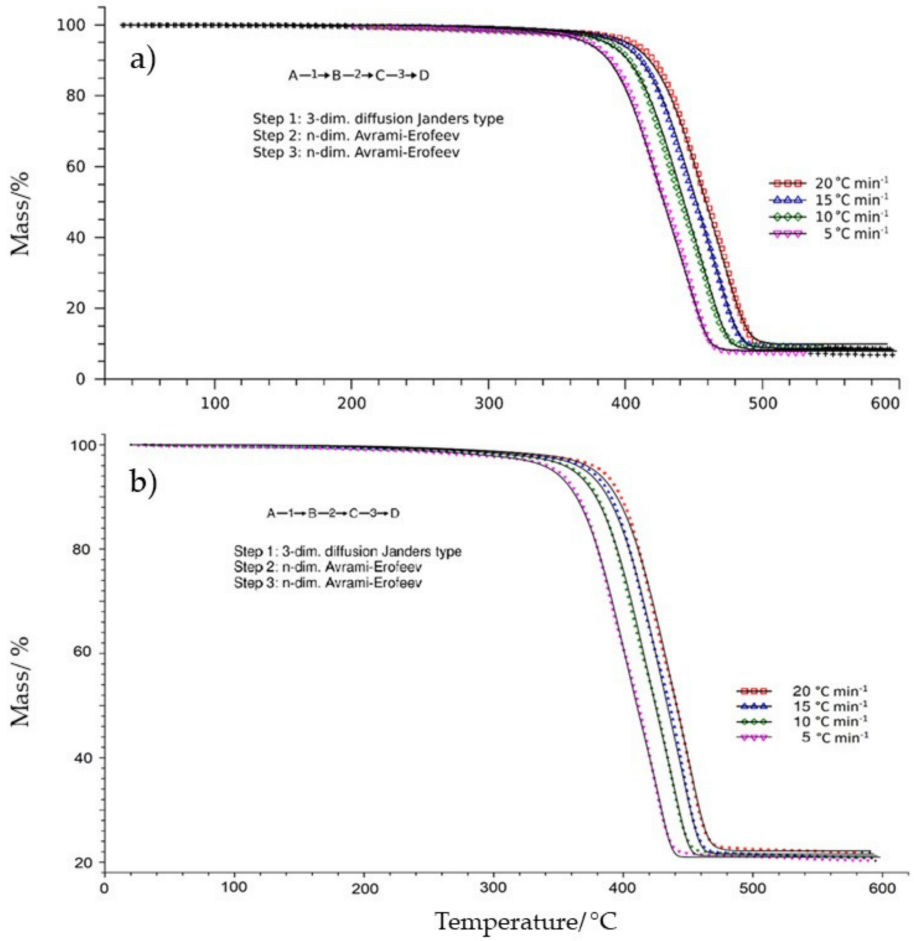

Figure 7. Graphical representation of non-linear regression model−fitting of the kinetic model (solid line) on the experimental points for (**a**) the mixture and (**b**) mixture with the catalyst.

All acquired information can be utilized to determine the operating conditions (residence time, temperature, and catalyst-to-polymer ratio) in a pilot-scale pyrolysis reactor to get the products (pyrolysis oil and gas) with the best potential for energy application.

4. Conclusions

The thermal and thermochemical behavior of the mixture, with or without the addition of a catalyst, was studied by carrying out TG experiments at different heating rates, and the decomposition mechanism was identified after a precise kinetic analysis supported by a well-established statistical procedure.

The findings of the TG/DTG measurements showed that the mixture of multi-layered plastic packaging degraded in at least two stages, with the maximum decomposition temperatures measuring between 350 and 510 °C (mass loss > 90%). The addition of a catalyst lowered the onset decomposition temperature of the mixture by about 24 °C.

The kinetic study of pyrolysis performed using the isoconversional Friedman method showed that the non-isothermal decomposition (namely, pyrolysis) of the examined mixture was a complex, multi-step process, regardless of the presence or absence of the catalyst. The activation energy values calculated by the Friedman method showed an increasing trend with the degree of conversion from 127 kJ mol^{-1} (at α = 0.01) to 219 kJ mol^{-1} (at α = 0.95). It is reasonable to assume that the E_{FR} values related to the processes occurring in the presence of the catalyst were lower by 44% and 8% for the first and the second steps, respectively, while they were substantially comparable for the third step. The evident enhancement of reactivity on the surface of the catalyst was reasonably ascribed to the doping of the catalyst with Iron(III). Consequently, the onset decomposition temperature in the presence of the catalyst was likewise reduced, as determined by TG analysis, resulting in less energy being required to heat the pyrolysis reactor.

Finally, we concluded that the aim of the study was achieved since the role of a ZSM-5 catalyst in the non-isothermal pyrolysis of a realistic waste mixture attributable to multi-layered plastic food packaging was substantially clarified.

Author Contributions: Conceptualization, I.K. and Z.H.-M.; methodology, I.K.; software, M.E.; validation, M.E.; formal analysis, M.E.; investigation, Z.K.; resources, Z.K.; data curation, S.V.C.; writing—original draft preparation, I.K., T.T., M.E., Z.H.-M., S.V.C. and D.R.S.; writing—review and editing, T.T., M.E., Z.H.-M. and S.V.C.; supervision, D.R.S.; project administration, I.K.; funding acquisition, D.R.S. All authors have read and agreed to the published version of the manuscript.

Funding: This research was funded by the Croatian Science Foundation under the project Neoplast (IP-2018-3200) and the project Career development for young researchers—training of new doctors of science (DOK-2018-09-6944). This support is gratefully acknowledged.

Data Availability Statement: The datasets generated during and/or analyzed during the current study are available from the corresponding author upon reasonable request.

Acknowledgments: The ZSM-5 zeolite catalyst was donated by Grace GmbH (Worms, Germany). This support is greatly appreciated.

Conflicts of Interest: The authors declare no conflict of interest.

References

1. Briassoulis, D.; Tserotas, P.; Hiskakis, M. Mechanical and degradation behaviour of multilayer barrier films. *Polym. Degrad. Stab.* **2017**, *143*, 214–230. [CrossRef]
2. PlasticsEurope. An Analysis of European Plastics Production, Demand and Waste Data. 2021. Available online: https://plasticseurope.org/knowledge-hub/plastics-the-facts-2021/ (accessed on 1 May 2022).
3. Mumladze, T.; Yousef, S.; Tatariants, M.; Kriukiene, R.; Makarevicius, V.; Lukošiute, S.I.; Bendikiene, R.; Denafas, G. Sustainable approach to recycling of multilayer flexible packaging using switchable hydrophilicity solvents. *Green Chem.* **2018**, *20*, 3604–3618. [CrossRef]
4. Morris, B.A. *The Science and Technology of Flexible Packaging: Multilayer Films from Resin and Process to End Use*; Elsevier: Amsterdam, The Netherlands, 2016.

5. Mount, E.M. Coextrusion Equipment for Multilayer Flat Films and Sheets. In *Multilayer Flexible Packaging*, 2nd ed.; Wagner, J.R., Jr., Ed.; Elsevier: Amsterdam, The Netherlands, 2016; pp. 99–122. [CrossRef]
6. Niaounakis, M. *Recycling of Flexible Plastic Packaging*; Elsevier: Amsterdam, The Netherlands, 2019. [CrossRef]
7. Thoden van Velzen, U.; Weert, L.; Molenveld, K. *Flexible Laminates within the Circular Economy*; Wageningen Food & Biobased Research: Wageningen, The Netherlands, 2020.
8. Mieth, A.; Simoneau, C.; Hoekstra, E. *Guidance for the Identification of Polymers in Multilayer Films Used in Food Contact Materials*; EUR 27816 EN; European Union: The Hague, The Netherlands, 2017. [CrossRef]
9. Anukiruthika, T.; Sethupathy, P.; Wilson, A.; Kashampur, K.; Moses, J.A.; Anandharamakrishnan, C. Multilayer packaging: Advances in preparation techniques and emerging food applications. *Compr. Rev. Food Sci. Food Saf.* **2020**, *19*, 1156–1186. [CrossRef] [PubMed]
10. Walker, T.W.; Frelka, N.; Shen, Z.; Chew, A.K.; Banick, J.; Grey, S.; Kim, M.S.; Dumesic, J.A.; Van Lehn, R.C.; Huber, G.W. Recycling of multilayer plastic packaging materials by solvent-targeted recovery and precipitation. *Sci. Adv.* **2020**, *6*, eaba7599. [CrossRef] [PubMed]
11. Kaiser, K.; Schmid, M.; Schlummer, M. Recycling of Polymer-Based Multilayer Packaging: A Review. *Recycling* **2018**, *3*, 1. [CrossRef]
12. Horodytska, O.; Valdés, F.J.; Fullana, A. Plastic flexible films waste management—A state of art review. *Waste Manag.* **2018**, *77*, 413–425. [CrossRef]
13. Conversio Market and Strategy GmbH. Global Plastics Flow 2018. 2020. Available online: https://www.carboliq.com/pdf/19_conversio_global_plastics_flow_2018_summary.pdf (accessed on 30 May 2022).
14. Tomić, T.; Schneider, D.R. The role of energy from waste in circular economy and closing the loop concept–Energy analysis approach. *Renew. Sustain. Energy Rev.* **2018**, *98*, 268–287. [CrossRef]
15. Tomić, T.; Schneider, D.R. Circular economy in waste management–Socio-economic effect of changes in waste management system structure. *J. Environ. Manag.* **2020**, *267*, 110564. [CrossRef]
16. De Mello Soares, C.T.; Ek, M.; Östmark, E.; Gällstedt, M.; Karlsson, S. Recycling of multi-material multilayer plastic packaging: Current trends and future scenarios. *Resour. Conserv. Recycl.* **2022**, *176*, 105905. [CrossRef]
17. Ragaert, K.; Delva, L.; Van Geem, K. Mechanical and chemical recycling of solid plastic waste. *Waste Manag.* **2017**, *69*, 24–58. [CrossRef]
18. Thiounn, T.; Smith, R.C. Advances and approaches for chemical recycling of plastic waste. *J. Polym. Sci.* **2020**, *58*, 1347–1364. [CrossRef]
19. Anuar Sharuddin, S.D.; Abnisa, F.; Wan Daud, W.M.A.; Aroua, M.K. A review on pyrolysis of plastic wastes. *Energy Convers. Manag.* **2016**, *115*, 308–326. [CrossRef]
20. Mark, L.O.; Cendejas, M.C.; Hermans, I. The Use of Heterogeneous Catalysis in the Chemical Valorization of Plastic Waste. *Chem. Sus. Chem.* **2020**, *13*, 5808–5836. [CrossRef] [PubMed]
21. Ratnasari, D.K.; Nahil, M.A.; Williams, P.T. Catalytic pyrolysis of waste plastics using staged catalysis for production of gasoline range hydrocarbon oils. *J. Anal. Appl. Pyrolysis* **2017**, *124*, 631–637. [CrossRef]
22. Miskolczi, N.; Sója, J.; Tulok, E. Thermo-catalytic two-step pyrolysis of real waste plastics from end of life vehicle. *J. Anal. Appl. Pyrolysis* **2017**, *128*, 1–12. [CrossRef]
23. Kassargy, C.; Awad, S.; Burnens, G.; Kahine, K.; Tazerout, M. Experimental study of catalytic pyrolysis of polyethylene and polypropylene over USY zeolite and separation to gasoline and diesel-like fuels. *J. Anal. Appl. Pyrolysis* **2017**, *127*, 31–37. [CrossRef]
24. Siddiqui, M.Z.; Park, Y.K.; Kang, Y.; Watanabe, A.; Kim, S.; Kim, Y.M. Effective use of aluminum-plastic laminate as a feedstock for catalytic pyrolysis over micro and mesoporous catalysts. *J. Clean. Prod.* **2019**, *229*, 1093–1101. [CrossRef]
25. Veksha, A.; Yin, K.; Moo, J.G.S.; Da Oh, W.; Ahamed, A.; Chen, W.Q.; Weerachanchai, P.; Giannis, A.; Lisak, G. Processing of flexible plastic packaging waste into pyrolysis oil and multi-walled carbon nanotubes for electrocatalytic oxygen reduction. *J. Hazard. Mater.* **2020**, *387*, 121256. [CrossRef]
26. Sivagami, K.; Divyapriya, G.; Selvaraj, R.; Madhiyazhagan, P.; Sriram, N.; Nambi, I. Catalytic pyrolysis of polyolefin and multilayer packaging based waste plastics: A pilot scale study. *Process Saf. Environ. Prot.* **2021**, *149*, 497–506. [CrossRef]
27. Yousef, S.; Eimontas, J.; Striūgas, N.; Zakarauskas, K.; Praspaliauskas, M.; Abdelnaby, M.A. Pyrolysis kinetic behavior and TG-FTIR-GC–MS analysis of metallised food packaging plastics. *Fuel* **2020**, *282*, 118737. [CrossRef]
28. Yousef, S.; Eimontas, J.; Zakarauskas, K.; Striūgas, N. Microcrystalline paraffin wax, biogas, carbon particles and aluminum recovery from metallised food packaging plastics using pyrolysis, mechanical and chemical treatments. *J. Clean. Prod.* **2021**, *290*, 125878. [CrossRef]
29. Eimontas, J.; Striūgas, N.; Abdelnaby, M.A.; Yousef, S. Catalytic pyrolysis kinetic behavior and TG-FTIR-GC–MS analysis of metallized food packaging plastics with different concentrations of ZSM-5 zeolite catalyst. *Polymers* **2021**, *13*, 702. [CrossRef] [PubMed]
30. Cafiero, L.; Fabbri, D.; Trinca, E.; Tuffi, R.; Vecchio Ciprioti, S. Thermal and spectroscopic (TG/DSC-FTIR) characterization of mixed plastics for materials and energy recovery under pyrolytic conditions. *J. Therm. Anal. Calorim.* **2015**, *121*, 1111–1119. [CrossRef]

31. Cafiero, L.; Castoldi, E.; Tuffi, R.; Vecchio Ciprioti, S. Identification and characterization of plastics from small appliances and kinetic analysis of their thermally activated pyrolysis. *Polym. Degrad. Stabil.* **2014**, *109*, 307–318. [CrossRef]
32. Benedetti, M.; Cafiero, L.; De Angelis, D.; Dell'Era, A.; Pasquali, M.; Stendardo, S.; Tuffi, R.; Vecchio Ciprioti, S. Pyrolysis of WEEE plastics using catalysts produced from fly ash of coal gasification. *Front. Environ. Sci. Eng.* **2017**, *11*, 11. [CrossRef]
33. Colantonio, S.; Cafiero, L.; De Angelis, D.; Ippolito, N.M.; Tuffi, R.; Vecchio Ciprioti, S. Thermal and catalytic pyrolysis of a synthetic mixture representative of packaging plastics residue. *Front. Chem. Sci. Eng.* **2020**, *14*, 288–303. [CrossRef]
34. Esposito, L.; Cafiero, L.; De Angelis, D.; Tuffi, R.; Vecchio Ciprioti, S. Valorization of the plastic residue from a WEEE treatment plant by pyrolysis. *Waste Manag.* **2020**, *112*, 1–10. [CrossRef]
35. Santella, C.; Cafiero, L.; De Angelis, D.; La Marca, F.; Tuffi, R.; Vecchio Ciprioti, S. Thermal and catalytic pyrolysis of a mixture of plastics from small waste electrical and electronic equipment (WEEE). *Waste Manag.* **2016**, *54*, 143–152. [CrossRef]
36. Al-Salem, S.M. Feedstock and optimal operation for plastics to fuel conversion in pyrolysis, Plast. to Energy Fuel. Chapter V. *Chem. Sustain. Implic.* **2018**, 117–146. [CrossRef]
37. Kremer, I.; Tomić, T.; Katančić, Z.; Erceg, M.; Papuga, S.; Parlov Vuković, J.; Schneider, D.R. Catalytic pyrolysis and kinetic study of real-world waste plastics: Multi-layered and mixed resin types of plastics. *Clean Technol. Environ. Policy* **2022**, *24*, 677–693. [CrossRef]
38. Vyazovkin, S.; Burnham, A.K.; Criado, J.M.; Pérez-Maqueda, L.A.; Popescu, C.; Sbirrazzuoli, N. ICTAC Kinetics Committee recommendations for performing kinetic computations on thermal analysis data. *Thermochim. Acta* **2011**, *520*, 1–19. [CrossRef]
39. Erceg, M.; Krešić, I.; Vrandečić, N.S.; Jakić, M. Different approaches to the kinetic analysis of thermal degradation of poly(ethylene oxide). *J. Therm. Anal. Calorim.* **2018**, *131*, 325–334. [CrossRef]
40. Qu, B.; Li, A.; Qu, Y.; Wang, T.; Zhang, Y.; Wang, X.; Gao, Y.; Fu, W.; Ji, G. Kinetic analysis of waste tire pyrolysis with metal oxide and zeolitic catalysts. *J. Anal. Appl. Pyrolysis* **2020**, *152*, 104949. [CrossRef]
41. Straka, P.; Bičáková, O.; Šupová, M. Thermal conversion of polyolefins/polystyrene ternary mixtures: Kinetics and pyrolysis on a laboratory and commercial scales. *J. Anal. Appl. Pyrolysis* **2017**, *128*, 196–207. [CrossRef]
42. Tao, L.; Ma, X.; Ye, L.; Jia, J.; Wang, L.; Ma, P.; Liu, J. Interactions of lignin and LDPE during catalytic co-pyrolysis: Thermal behavior and kinetics study by TG-FTIR. *J. Anal. Appl. Pyrolysis* **2021**, *158*, 105267. [CrossRef]
43. Liu, G.; Liao, Y.; Guo, S.; Ma, X.; Zeng, C.; Wu, J. Thermal behavior and kinetics of municipal solid waste during pyrolysis and combustion process. *Appl. Therm. Eng.* **2016**, *98*, 400–408. [CrossRef]
44. Vyazovkin, S.; Chrissafis, K.; Di Lorenzo, M.L.; Koga, N.; Pijolat, M.; Roduit, B.; Sbirrazzuoli, N.; Suñol, J.J. ICTAC Kinetics Committee recommendations for collecting experimental thermal analysis data for kinetic computations. *Thermochim. Acta.* **2014**, *590*, 1–23. [CrossRef]
45. Netzsch Gerätebau GmbH. *Netzsch Thermokinetics Software Manual*; Netzsch Gerätebau GmbH: Waldkraiburg, Germany, 2014.
46. Das, P.; Tiwari, P. Thermal degradation study of waste polyethylene terephthalate (PET) under inert and oxidative environments. *Thermochim. Acta* **2019**, *679*, 178340. [CrossRef]
47. Diaz Silvarrey, L.S.; Phan, A.N. Kinetic study of municipal plastic waste. *Int. J. Hydrogen Energy* **2016**, *41*, 16352–16364. [CrossRef]
48. Abnisa, F.; Wan Daud, W.M.A. A review on co-pyrolysis of biomass: An optional technique to obtain a high-grade pyrolysis oil. *Energy Convers. Manag.* **2014**, *87*, 71–85. [CrossRef]
49. Raveh-Amit, H.; Lemont, F.; Bar-Nes, G.; Klein-BenDavid, O.; Banano, N.; Gelfer, S.; Charvin, P.; Bin Rozaini, T.; Sedan, J.; Rousset, F. Catalytic Pyrolysis of High-Density Polyethylene: Decomposition Efficiency and Kinetics. *Catalysts* **2022**, *12*, 140. [CrossRef]
50. Sethia, G.; Dangi, G.P.; Jetwani, A.L.; Somani, R.S.; Bajaj, H.C.; Jasra, R.V. Equilibrium and dynamic adsorption of carbon monoxide and nitrogen on ZSM-5 with different SiO_2/Al_2O_3 ratio. *Sep. Sci. Technol.* **2010**, *45*, 413–420. [CrossRef]
51. Lv, H.; Zhang, Z.; Fan, L.; Gao, Y.; Zhang, X. A nanocaged cadmium-organic framework with high catalytic activity on the chemical fixation of CO_2 and deacetalization-knoevenagel condensation. *Microporous Mesoporous Mater.* **2022**, *335*, 111791. [CrossRef]